TOXICOLOGY AND APPLIED PHARMACOLOGY **109,** 276–288 (1991)

A Model for the Uptake of Inhaled Vapors in the Nose of the Dog during Cyclic Breathing[1]

PER GERDE AND ALAN R. DAHL

Inhalation Toxicology Research Institute, Lovelace Biomedical and Environmental Research Institute, P.O. Box 5890, Albuquerque, New Mexico 87185

Received January 16, 1991; accepted April 14, 1991

A Model for the Uptake of Inhaled Vapors in the Nose of the Dog during Cyclic Breathing. GERDE, P., AND DAHL, A. R. (1991). *Toxicol. Appl. Pharmacol.* **109,** 276–288. A model was developed to simulate the uptake of inhaled vapors in the nasal airway of the Beagle dog during cyclic breathing. Input data to the model were morphological and physiological data for the dog, and physiocochemical data for the vapors. The model simulates the nasal airway as a slit-like duct, where air passes between the two airway walls in an ideal plug flow. The thickness of the walls corresponds to the distance between the air interface and the average position where vapor molecules are removed into the capillary blood. All resistance to radial mass transfer is assumed to arise on the liquid side in the diffusion of vapors through the air/blood tissue barrier and in transport by the blood. The model results agreed reasonably well with experimental data. The nasal absorption of vapors on inhalation increased from 1% for a compound with a blood/air partition coefficient of 1 to around 95% uptake for a compound with a partition coefficient of 2000. Desorption from the nasal tissues on exhalation increased from approximately 1% to approximately 30% over the same range of partition coefficients. The nasal uptake over one complete breathing cycle, defined as absorption on inhalation minus desorption on exhalation, was almost zero for low partition coefficient compounds and plateaued at around 65% for high partition coefficient compounds. The model indicates that diffusional resistance and inertia of the nasal tissues result in temporary storage of absorbed vapors upon inhalation, followed by desorption of vapors back into the airstream upon exhalation. An important consequence of this phenomenon is a shift in exposure to inhaled vapors from the lungs to the nasal airway during cyclic flow compared with predictions from experiments and models based on unidirectional flow.

The nasal passages condition inhaled air and they are the first line of defense against airborne infectious or toxic agents (Brain, 1970; Morgan and Frank, 1977; Proctor and Swift, 1977). The uptake of inhaled toxic agents—including aerosols, gases, and vapors—has been studied both experimentally and theoretically. Because particles rarely reentrain into the air once deposited on the airway walls, particle deposition models are focused entirely on events in the gas phase of the lumen. This is equivalent to assuming as a boundary condition for the model equations that the particle concentration at the airway wall is zero (Yeh, 1974). When gases and vapors are deposited, this assumption is rarely warranted. Most often, deposited molecules can reentrain into the airways and, thus, exert a back pressure at the airway wall. This back pressure depends heavily on events in the liquids of the mucus layer and the tissue below. Therefore, processes on the liquid tissue side are likely to be equally important, in determining the uptake of inhaled gases and vapors than are processes in the gas phase of the lumen.

[1] The U.S. Government's right to retain a nonexclusive royalty-free license in and to the copyright covering this paper, for governmental purposes, is acknowledged.

0041-008X/91 $3.00

TABLE 1

OVERVIEW OF CURRENT MODELS DESCRIBING NASAL UPTAKE OF VAPORS

Model	Major compartments/ transport mechanisms[a]	Contact pattern[b]	Flow regime[c]
LaBelle *et al.* (1955)	Air/blood conv/conv	Tank reactor	Unidirectional
Aharonson *et al.* (1974)	Air/tissue/blood conv//conv	Tube reactor	Unidirectional
Corn *et al.* (1976)	Air/tissue conv and diff//	Tube reactor	Unidirectional
Morris and Cavanagh (1986)	Air/blood conv/conv	Tank reactor	Unidirectional
Stott *et al.* (1986)	Air/blood conv/conv	Tank reactor	Unidirectional
This model	Air/tissue/blood conv/diff/conv	Tube reactor	Cyclic

[a] Refers to the assumed principal physicochemical transport mechanism, which is either convection or diffusion. "/" indicates a simple equilibrium at an interface, whereas "//" indicates a more complicated relation for transport across the interface.

[b] Indicates if the air is either in contact with the airway wall as in a well-stirred tank reactor or if it flows along the airway wall as in a tube reactor.

[c] Distinguishes between models assuming a constant, one-way inspiratory flow, and models assuming a sinusoidally varying, cyclic flow.

Several papers have discussed the general principles for vapor uptake in the respiratory tract (Morgan and Frank, 1977; Overton, 1984; Hanna *et al.*, 1985; Ultman, 1986). Uptake of gases and vapors in the respiratory region involves gas/liquid interfacial transport, and the importance of the liquid/air partition coefficient for uptake was recognized early (Henderson and Haggard, 1943; La Belle *et al.*, 1955): the higher the partition coefficient (PC), the higher the nasal uptake. Interfacial transport processes have been treated extensively in engineering literature (Bird *et al.*, 1960). A gas/liquid interfacial transport involves two separate resistances connected in series: the gas phase resistance and the liquid phase resistance. "Resistance" in this sense refers to a slowing of transport, for example, as a result of limiting diffusion rates. Usually the resistance at the interface (e.g., the boundary between the gas phase and the tissue phase) is assumed to be zero, and the concentrations on both sides of the interface are assumed to be equilibrium with each other. This approach has been used to model the uptake of gases and vapors in the respiratory tract, particularly in the pulmonary airways (DuBois and Rogers, 1968; Davidson and Schroter, 1983; Miller *et al.*, 1985).

In the nasal airway, the interfacial transport connects the resistance in the gas phase with the resistance on the liquid tissue side. In the gas phase, axial transport in the airway occurs with bulk movement of the air and through turbulent and diffusional dispersion, while radial transport occurs mostly through diffusion. The dominating mode of transport in the liquid (i.e., tissue) phase is radial diffusion through the mucosa to the capillaries.

The few models describing uptake of gases and vapors by the nasal airway (Table 1) can be divided into broad categories according to their major properties: property 1, the major compartments (e.g., air, mucus/tissue, and blood) that are involved; property 2, the mechanisms used to describe transport (con-

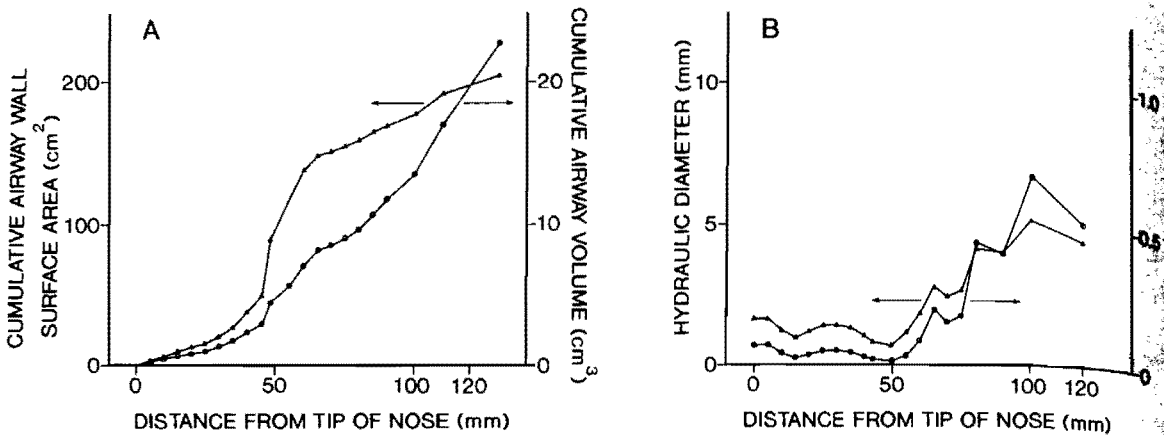

FIG. 1. Critical dimensions of the nasal airway of the Beagle dog used in the model (Schreider and Raabe, 1981). (A) Cumulative surface area of the airway wall, and cumulative airway volume with distance from the tip of the nose. (B) The hydraulic diameter and corresponding diffusional relaxation time of the airspace as a function of distance into the nose. The relaxation time is the time it takes for molecular diffusion to even out radial concentration gradients in the airspace.

vection or diffusion); property 3, the contact pattern assumed between air and airway walls (the two extremes are the tank reactor, with a total backmixing of the air in contact with the airway wall, and the tube reactor, with a flow of air along the airway wall); property 4, the airflow regime (either undirectional flow or sinusoidally varying cyclic flow).

The purpose of this study was to develop a model for predicting the uptake of stable vapors in the nasal airway of the Beagle dog under cyclic breathing conditions and to compare predictions with results of parallel experiments in the same species. The results of the experiments are published in a companion article in this tissue (Dahl *et al.*, 1991). Input data for the model were intentionally limited to morphological and physiological parameters for the dog and physicochemical parameters for the vapors. In addition, the experimentally derived concentrations of vapor exhaled from the lungs into the nasal airway were used as input to the model.

MODEL CONSTRUCTION

The morphology of the nasal airway has been mapped in several species of laboratory animals using airway casts (Schreider and Raabe, 1981) and in humans using magnetic resonance imaging (Guilmette *et al.*, 1989). Proceeding caudally in the dog, the cross section of the nasal airway takes the shape of two slit-like ducts in the nares that branch in the turbinates and abruptly form a circular duct in the nasopharynx. The slit-like duct in the turbinate region has a considerably smaller width than the airways posterior to the pharynx, until the point within the lung at which a high degree of branching is reached (Proctor and Swift, 1977). Figure 1A shows the cumulative wall surface area and the cumulative volume of the nasal airway of the Beagle dog as a function of position along the nasal airway. The hydraulic diameter is a useful concept to describe heat and mass transfer to the walls of noncircular ducts, like the nasal airway. Therefore, the hydraulic diameter can be used to estimate the relative resistance to mass transfer in the gas phase compared with resistance on the liquid tissue side. It is defined as twice the cross-sectional area of a duct divided by its perimeter (Bird *et al.*, 1960). The smaller the hydraulic diameter, that is, the larger the wall surface area compared with the volume of the duct, the more rapid the heat–mass transfer to the walls of the duct. Figure 1B shows the calculated hydraulic diameter as a function of position along the nasal airway of

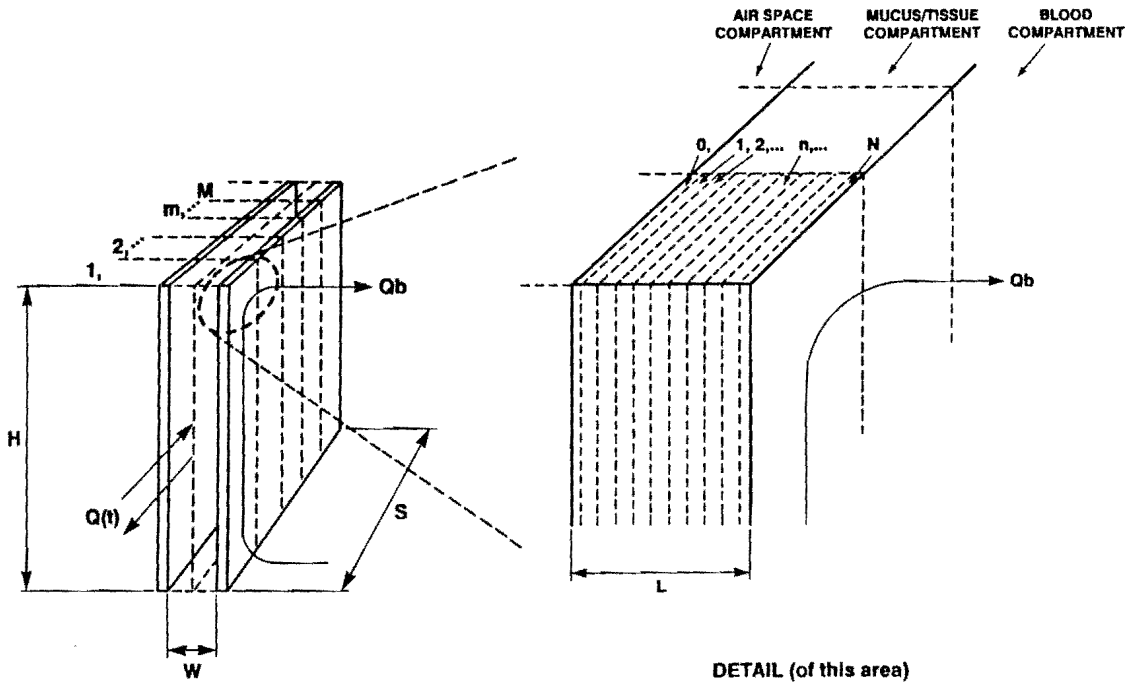

FIG. 2. A schematic view of the nasal airway model consisting of two vertical parallel plates. Air passes in the gap between the plates in a cyclic flow $Q(t)$, and the thickness of the plates corresponds to the average distance between the air and the capillary blood of the nasal airway. Blood perfuses the outside of the mucus/tissue plates at a flow rate Q_b. For definitions of letters, see Table 2.

the Beagle dog. The morphometric data are from Schreider and Raabe (1981).

The hydraulic diameter can be used to estimate radial transfer rates of gases and vapors in the different regions of the respiratory tract. If a stagnant fluid is assumed, a conservative estimate of the radial transport capacity in the gas phase is obtained if the hydraulic diameter is used to calculate the characteristic time required for molecular diffusion to even out any radial concentration gradients within different sections of the airways. The diffusivity of small organic molecules at 37°C in air was estimated from Perry *et al.* (1963) to be about 1.0×10^{-5} (m^2/sec). In a rectangular slit-like duct, the hydraulic diameter approximates the width of the duct. The rate at which a stagnant fluid will attain equilibrium through diffusion can then be obtained from the solution of the case where a solute diffuses in a plane sheet (Crank, 1975). Figure 1B shows the characteristic time required to attain 90% of the equilibrium concentration in various sections of the nasal airway (the relaxation time). In reality, the transfer rate is considerably faster because of the turbulent mixing of the air during breathing. This is indicated by the high Sherwood's numbers that have been obtained in experiments with nasal casts (Hanna *et al.*, 1985; Hanna and Scherer, 1986). The Sherwood's number is a dimensionless parameter that characterizes mass transfer in a streaming fluid. The higher the Sherwood's number, the faster the rate of mass transfer in a streaming fluid than in a stagnant fluid.

We have simulated the turbinate region of the Beagle dog as one slit-like duct between two vertical parallel plates (Fig. 2), a concept that has been used by others for particle deposition models (Scott *et al.*, 1978; Bailey, 1984). Inhaled air passes through the gap between the plates. The surface area of the plates corresponds to the cumulative surface area of the turbinate region down to the pharynx, and the gap (W in Fig. 2) between the plates corresponds to the width of the airway duct or the average hydraulic diameter of the turbinate region. The thickness of the plates corresponds

to the average thickness of the air/blood barrier. This is the distance between the air interface and the average position where vapor molecules are removed by the capillary blood of the nasal airway mucosa.

Air passes between the plates in an ideal plug flow, and the flow rate varies sinusoidally over time. Because of the efficient radial air phase transport in the nasal airway (Hanna *et al.*, 1985), we have assumed that, for the range of PC simulated, the air is instantaneously equilibrated with the tissue/air interface, and, thus all resistance to mass transfer is assumed to be on the liquid side. The vapor molecules diffuse through the mucous lining and the mucosa to the capillaries below, thus establishing a concentration profile through the tissue barrier that changes over the breathing cycle.

A considerable diffusional resistance on the tissue side of the air/tissue interface was demonstrated in a unidirectional flow experiment by Aharonson *et al.* (1974). The concentration of acetone downstream from the nasal region in a dog was measured during the beginning of the experiment. Some 20 sec were required for the concentration to rise from zero to a quasi-steady-state level. Most likely, this "missing" amount of acetone was involved in establishing a concentration gradient from the air interface to the capillary net of the nasal mucosa. The experiment also demonstrated the rapid attainment of quasi-steady-state during unidirectional flow, even for a high PC compound like acetone (blood/air PC 245; Sato and Nakajima, 1979).

In the model presented here, vapor uptake in the Beagle dog turbinate region has been simulated using a simplified numerical scheme (See Appendix). This was accomplished by dividing the region containing one of the model airway walls (from the tissue/blood interface to the symmetry line in the airspace between the plates) into three compartments: the airspace compartment, the mucus/tissue compartment, and the blood compartment (Fig. 2). The tissue compartment was further divided into M sections of equal size along the direction of inspiratory flow, and each tissue section was divided into N equally spaced nodes with depth from the air interface toward the tissue/blood interface. Transport of vapors was assumed to occur in the gas phase only through convective flow along the duct and radially through the tissues by means of molecular diffusion. The problem was solved by the method of fractional steps (Press *et al.*, 1986). The concentration in each section of the gas phase was assumed to be instantaneously equilibrated with its neighboring tissue node. For each time step, the concentrations in the M sections of the gas phase and the M interfacial tissue nodes were calculated. The radial transport through the M arrays of N tissue nodes was then solved.

The concentration of vapor in the inhaled air was normalized to 1. The tissue/blood interface was assumed to cover the whole outside of the tissue plate, and each node at the tissue/blood interface was presented with fresh blood of zero vapor concentration (Brain, 1970). This assumption was strengthened by experimental results (Dahl *et al.*, 1991), in which, with the possible exception of dimethyl pentane, no indication of back pressure from systemic circulation was observed with the compounds modeled during 10- to 30-min exposures. Based on the observation of a substantial bloodborne vapor removal from the nasal airway, as indicated by unidirectional, ventilation–perfusion models (Stott *et al.*, 1986; Morris and Cavanagh, 1986), it was assumed that the exiting blood was in equilibrium with the neighboring tissue node at the blood/mucosa interface. Table 1 compares our model with earlier models.

SIMULATION

Two critical input parameters for the model are the average thickness of the air/blood barrier and the average blood flow removing the vapor from the nasal mucosa (Table 2). Important information on the latter parameter can be obtained from Morris and Cavanagh

TABLE 2

PHYSIOLOGICAL AND PHYSIOCHEMICAL DATA FOR DOG MODEL

Nasal airway dimensions[a]	
Length of airway duct S (m):[b]	0.10
Height of airway duct H (m):[b]	0.105
Width of airway duct W (m):[b]	2.2×10^{-3}
Thickness of air/blood tissue barrier L (m):[c]	60×10^{-6}
Breathing and perfusion characteristics	
Tidal volume (m^3):[d]	300×10^{-6}
Breathing frequency (min^{-1}):[d]	14.0
Perfusion rate Q_b ($m^3/m^2/sec$):[e]	1.6×10^{-5}
Vapor properties	
Diffusivity in tissues D (m^2/sec):[f]	0.5×10^{-9}
Blood/air partition coefficients K_{pc} (vol/vol):[d]	1–2000
Blood/tissue partition coefficients:[g]	1.0
Average concentration of vapor exhaled from lung:[d]	From experiments

[a] See Fig. 2.
[b] Based on data from Schreider and Raabe (1981).
[c] Derived in this paper.
[d] Obtained from experiments. Dahl *et al.* (1991).
[e] Estimated from Morris and Cavanagh (1986), Pfeffer and Frohlich (1972), and Muggenburg and Mauderly (1974).
[f] Estimated from Perry *et al.* (1963) and Lightfoot (1974).
[g] Assumed approximation.

(1986). Measuring nasal uptake of vapors in the rat under unidirectional flow, Morris and Cavanagh concluded that about 0.7% of the cardiac output of the rat (Pfeffer and Frohlich, 1972) was instrumental in removing the vapor from the nasal region. Because the turbinate region of the dog has a degree of complexity similar to that of the rat, it may be assumed that the same percentage of the cardiac output (Muggenburg and Mauderly, 1974) is involved in removing vapors in the Beagle dog. This would give a blood flow of 20 ml/min.

The average diffusivity of the test vapors in tissues was estimated in the following way. The average diffusivity in water for solutes of similar molecular weight to the ones simulated was estimated from Perry *et al.* (1963) to be 0.9×10^{-9} (m^2/sec). By comparison, Lightfoot (1974) gave the diffusivity for oxygen in water and tissues at 37°C to be 2.5×10^{-9} and 1.4×10^{-9} (m^2/sec), respectively. Assuming that the same reduction in diffusivity in tissues relative to that in water occurs for the test vapors, an average tissue diffusivity of 0.5×10^{-9} (m^2/sec) was derived.

The most difficult parameter to obtain was the average air/blood barrier thickness of the nasal mucosa. The nasal mucosa of the dog is a well-perfused organ. The capillaries are normally found immediately below the epithelium, where blood vessel lumens make up between 17 and 43% of the tissue volume (Adams and Hotchkiss, 1983). The thickness of the canine respiratory epithelium, which covers a large portion of the turbinate region, ranges from 16 to 80 μm, and the distance to the most superficial capillaries is 12–18 μm (Adams and Hotchkiss, 1983). Because of the greater variability in the nasal airway vascularization, a crude optimization was made by varying this parameter to fit with the experimental data (Dahl *et al.*, 1991). The desired parameter was the average distance from the air interface to the position where the vapor molecules are removed with the blood. This distance exceeds the distance to the most su-

perficial capillaries. The optimization gave a distance of 60 μm.

The vapor uptake was simulated over eight full breathing cycles, starting with inhalation and zero concentration of vapor within the model compartments. The vapor concentration of various elements in the model was compared at the same sinusoidal phase angle in the last two cycles, and uptake was calculated during the last cycle. Nasal absorption is defined as the fraction of the inhaled vapor taken up by the nasal mucosa during the inhalation phase of the breathing cycle. Nasal desorption is the fraction of the inhaled vapor released to the exhaled air on passage through the nasal region. Lung uptake is defined as the fraction of the total inhaled vapor taken up by the lungs. Finally, nasal uptake, or the bloodborne removal of vapors from the nose, is defined as nasal absorption minus nasal desorption.

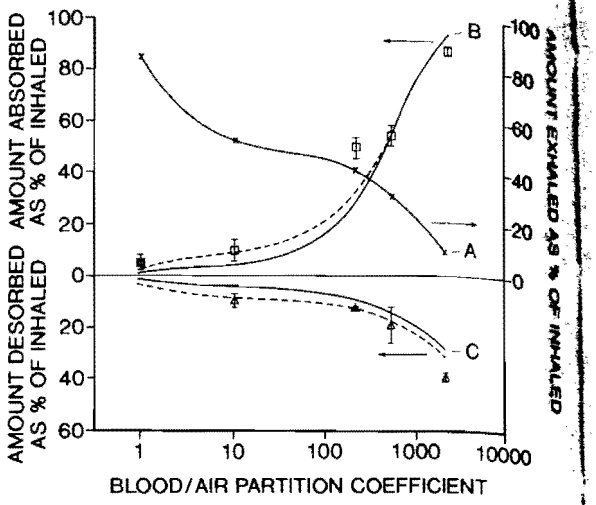

FIG. 3. The simulated uptake of vapors in the nasal airway of the Beagle dog during cyclic breathing as a function of the blood/air partition coefficient. The simulation results are shown together with experimental data for whole-breath uptake of vapors. Curve A, Amount exhaled from the lung, derived from the experimental data (Dahl *et al.*, 1991), was used as input to the model. Curve B, Nasal absorption on inhalation. Curve C, Nasal desorption on exhalation. Dashed lines show the simulated effect of the constant sampling flow rate over the breathing cycle that was used in collecting the experimental data (Dahl *et al.*, 1991). Experimental data are shown for the following vapors, given in the order of increasing PC: 2,4-dimethyl pentane, propyl ether, butanone, dioxolane, and ethanol. Error bars represent standard error of the means.

RESULTS

The model predicts that the uptake of vapors in the nasal region of the dog is highly dependent on the liquid/air PC. All simulations were done with the blood/air PC, which yielded a better fit with the experimental data than did the air/water PC (Dahl *et al.*, 1991). In Fig. 3, the model simulations are shown as solid lines together with the experimental data points. The nasal absorption on inhalation increases from about 1% at a PC of 1 to almost 95% at a PC of around 2000. The nasal desorption of vapors ranges from about 1% to about 30%, giving a total bloodborne uptake in the nose of about 65%. Thus, less than 100% uptake in the nasal airway does not indicate incomplete absorption, because a portion of the vapor absorbed in the nasal airway during inhalation is subsequently desorbed during exhalation.

The simulated vapor concentrations in air after passing through the nasal cavity during inhalation and exhalation are shown in Fig. 4. Simulations were made for compounds having high (PC = 2000), medium (PC = 200), or low (PC = 1) blood/air PCs. For a high PC compound, the absorption of vapor, indicated by the difference between nose and tracheal concentrations, was predicted to occur over the entire inhalation phase (Fig. 4A), whereas, for a low PC compound, absorption was predicted to occur rapidly—almost immediately after the flow reverses (Fig. 4C). The higher the PC, the larger the air volume that is needed to effect significant change in the vapor concentration in the nasal mucosal tissues. Desorption during the exhalation phase, indicated by the difference between the tracheal and the nose concentrations, we predicted to occur in the early part of the exhalation phase for the entire range of PC simulated. The uneven absorption and desorption over the breathing cycle pointed toward a potential experimental problem. In the experimental ap-

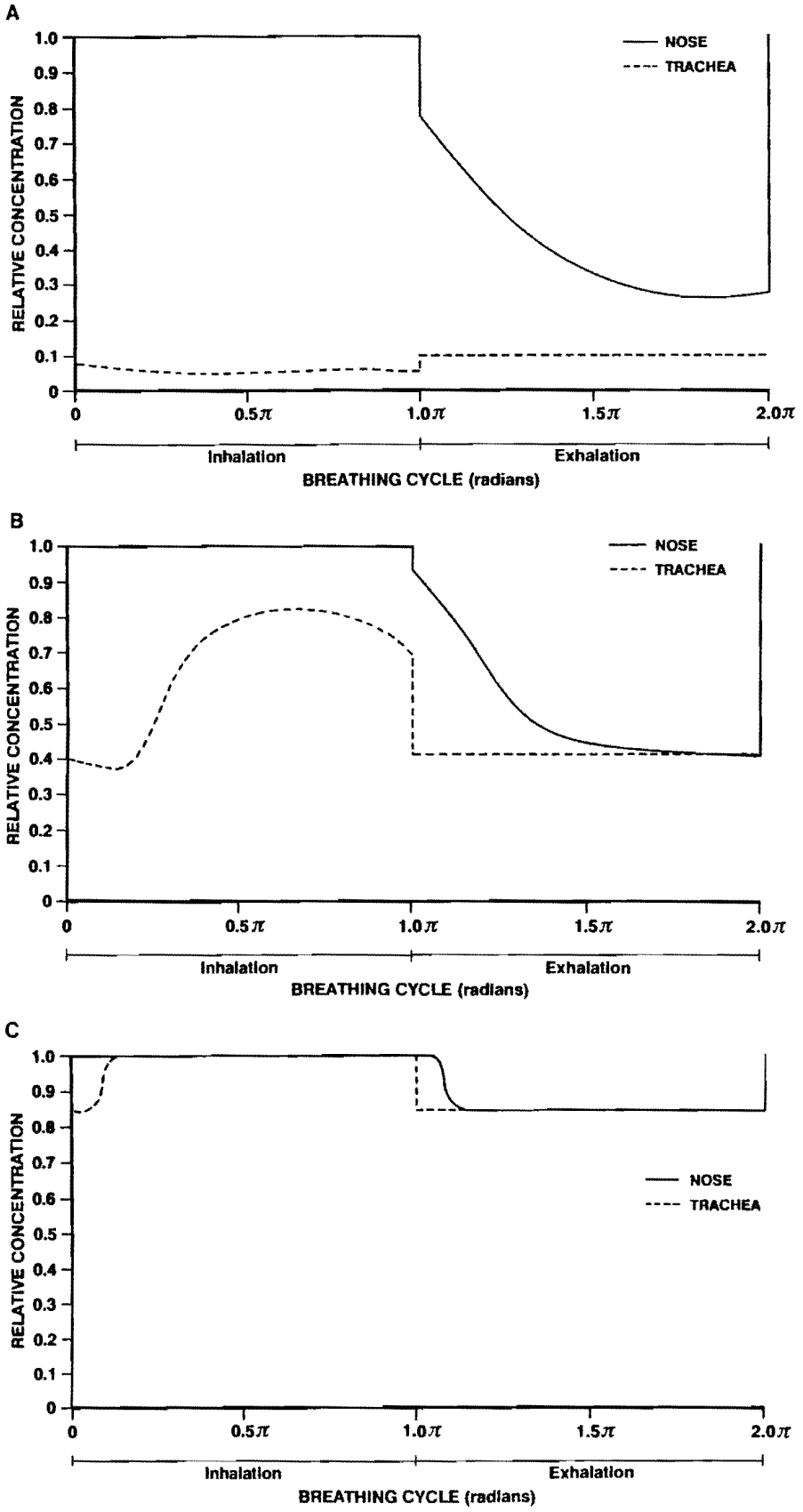

FIG. 4. Simulated concentrations of vapor at the tip of the nose and in the trachea during one full breathing cycle. (A) High blood/air partition coefficient compound (PC = 2000). (B) Intermediary partition coefficient (PC = 200). (C) Low partition coefficient compound (PC = 1).

proach (Dahl *et al.*, 1991), air was sampled to the gas chromatograph at a constant flow rate over the breathing cycle (Snipes *et al.*, 1991), whereas the breathing flow rate varied sinusoidally. The sampling strategy used in the experiments tended to overemphasize the vapor concentration when the breathing flow rate was lowest, which occurs near the point of reversal of flow. The effect of a constant sampling flow rate on absorption and desorption of vapors was simulated in the model, and the results are shown as dashed lines in Fig. 3. The dashed lines should, thus, give the best fit with the uncorrected experimental data, which were derived using a constant sampling flow rate over the whole breath of the dog (Dahl *et al.*, 1991). As expected, the constant sampling flow rate gave the largest errors for low PC compounds. Both the measured nasal absorption and nasal desorption, albeit low, could be two times the correct value for a compound with a PC of 1. A similar, but coarser, correction for the constant sampling flow rate was made directly on the experimental data (Dahl *et al.*, 1991).

DISCUSSION

Model simulations indicate that the uptake of vapors in the nasal region during cyclic flow is qualitatively different than that during experimentally created unidirectional flow. In general, less vapor is likely to pass the nasal region and continue into the lungs during cyclic flow than would be predicted from unidirectional flow data and models. The reason for this is the considerable diffusional resistance and inertia of the air/blood barrier of the nasal airway, which give the nasal mucosa a temporary storage capacity. On inhalation, vapors will dissolve in the lining layer liquids at the air interface and will gradually establish a concentration gradient toward the capillary bed of the mucosa. When the airflow reverses and air exits the lungs, the direction of diffusion reverses, and a fraction of what is dissolved in nasal mucus, as well as in the underlying mucosa, will diffuse back to the air interface and desorb into the exhaled air. The vapor molecules absorbed during inhalation simply do not have time to pass into the blood before they reentrain into the air stream upon exhalation. In contrast, during unidirectional flow, the mucosa will not be given time to desorb and will rapidly attain a comparatively high and constant vapor concentration at the air interface, and more vapor will be passed onto the lungs because the nasal absorption capacity is not renewed by desorption. Therefore, during cyclic flow, the nasal region is likely to absorb a larger fraction, and the lungs will receive a smaller fraction of inhaled vapors than would be predicted based on hypothetical, unidirectional flow. This effect will be most pronounced for compounds having high PCs, for which the lungs experience very little exposure to the vapors during cyclic flow (Dahl *et al.*, 1991).

The results of the model simulations agreed well with the experimental data, especially considering the relative simplicity of the model and the fact that only physically or physiologically relevant parameters were used as input data. The good agreement between experimental results and model predictions supports our assumptions regarding the physicochemical nature of the mechanism influencing nasal uptake of vapors. The model also provides interesting predictions on the relative influence of the gas, tissue, and blood compartments on nasal uptake. Vapors of compounds having very high PCs should be rapidly removed from the inhaled air by absorption in the anterior part of the nasal cavity. For such compounds, air flow patterns should have an important influence on the local nasal tissue dose (Morgan and Monticello, 1990). When the PC of the compound under consideration is low enough that the vapor breaks through to the lungs, however, nasal absorption and uptake of the vapor are also highly dependent on the rate of diffusion of the vapor through the tissue barrier between the gas phase and the capillaries. The shorter the distance of diffusion and the higher the perfusion rate, the lower the local dose to

the nasal tissues. For vapors with relatively low PCs, the entire surface of the nasal cavity will be exposed to nearly the same air concentration of vapor, and systemic uptake of vapor from the nasal cavity will depend almost completely on perfusion and rate of diffusion through the tissue barrier separating inhaled air from the capillaries. We note that the relative importance of airflow patterns and perfusion and diffusion rates will change gradually with changes in the PC of the vapor under consideration. Thus, all-or-none categorization of vapors, such as is implied with terms like "soluble" and "insoluble," are inappropriate.

The two major model simplifications are the zero resistance and zero axial dispersion in the gas phase. If the PC of an inhaled vapor is high enough that there is no substantial back pressure from absorbed vapor, there will be a steep concentration gradient from the center of the lumen to the air/tissue interface, and the simplification of zero resistance in the gas phase may lead to overestimation of the nasal uptake. Experimental data for ethanol (PC ~2000) (Dahl *et al.*, 1991) indicate that, for this vapor, sufficient back pressure from the tissues occurs to allow measurable penetration through the nasal airway, which indicates, in turn, that the liquid side resistance is considerable. Thus, for gas phase resistance to become important relative to liquid phase resistance in the dog nasal airway, the PC of the vapor under consideration must exceed approximately 2000.

Our model can be used to help design experiments to determine vapor uptake. For example, the model indicates that experimental data will be most difficult to collect for low PC compounds, because only a small amount of vapor is taken up on inhalation and is subsequently desorbed from the nasal airway. The mass transfer for such vapors should occur immediately after the breathing flow reverses, which for the experimental techniques used by Snipes *et al.* (1991) should be overrepresented by the constant sampling flow rate used (Dahl *et al.*, 1991).

CONCLUSIONS

Uptake of "stable" (Dahl, 1990) vapors by the nasal region is essentially a physicochemical process. The main parameters influencing uptake are the tissue/air PC of the vapor; the breathing characteristics of the subject; the airway dimensions and surface area; the thickness of the air/blood tissue barrier; and the perfusion rate of the nasal mucosa.

In the dog, there is a shift from compounds with a PC of less than 1—where almost nothing is taken up by the nasal region, and most of the uptake is in the lungs—to compounds with a PC of larger than 2000—where most of the vapor is taken up in the nose and little reaches the lungs.

Because of the diffusional resistance and inertia of the nasal mucosa, cyclic flow leads to the temporary storage of absorbed vapors in nasal tissues on inhalation, followed by desorption of vapors on exhalation. Cyclic flow, in contrast to unidirectional flow, simply does not provide sufficient time for all of the absorbed vapor molecules to reach the bloodstream before reentrainment into the exhaled air. This phenomenon shifts the exposure to vapors during cyclic flow from the lungs to the nasal airway, compared with predictions based on hypothetical unidirectional flow.

APPENDIX: DERIVATION OF THE MODEL EQUATIONS

The model consists of three coupled compartments: the airspace compartment; the mucus/tissue compartment; and the blood compartment (see Fig. 2). All three compartments are sliced perpendicularly to the airflow vector into M sections of equal width. In addition, the tissue part of these sections is each divided into N nodes of equal size.

C_g (g/m^3) is the vapor concentration in the air; C (g/m^3) is the concentration of the dissolved vapor in the tissue compartment; and finally, C_b (g/m^3) is the vapor concentration in the blood compartment.

The Air Space Compartment

Air enters between the model plates at a sinusoidally varying flow rate given by

$$Q = Q_{max}\sin(\omega t),$$

where Q_{max} is the maximum inspiratory flow rate (m^3/sec), ω is the breathing rate expressed as angular speed (rad/sec), and t is time (sec). The vapor concentration in the inspired air is constant and normalized to $C_{gin} = 1.0$. The vapor concentration in the air exhaled from the lungs into the nasal region C_{gex} was taken from the experimental data and was assumed to be constant over the exhalation part of the breathing cycle. The M sections of the airspace compartment are stored in the matrix $C_{g(2,M)}$. Index 2 refers to the concentrations of two adjacent time steps necessary to store when solving the problem numerically.

On inhalation, the concentration (C_g) in the first airspace section after the lapse of one time step dt is given by

$$C_{g(2,1)} = \frac{QC_{gin}dt + (dV - Qdt)C_{g(1,1)} + dAdL/2C_{(0,1,1)}}{dV + K_{pc}dAdL/2},$$

and similarly for the second through Mth airspace section,

$$C_{g(2,m)} = \frac{QC_{g(1,m-1)}dt + (dV - Qdt)C_{g(1,m)} + dAdL/2C_{(0,1,m)}}{dV + K_{pc}dAdL/2},$$

where K_{pc} is the tissue/air partition coefficient (volume/volume). On exhalation, the change in concentration in the first through $(M-1)$th airspace after the lapse of one time step will be

$$C_{g(2,m)} = \frac{(dV - Qdt)C_{g(1,m)} - QC_{g(1,m-1)}dt + dAdL/2C_{(0,1,m)}}{dV + K_{pc}dAdL/2},$$

and similarly for the Mth air space section,

$$C_{g(2,M)} = \frac{(dV + Qdt)C_{g(1,M)} - QC_{gex}dt + dAdL/2C_{(0,1,M)}}{dV + K_{pc}dAdL/2}$$

The new concentrations in the M tissue nodes facing the airspace can then be calculated through

$$C_{(0,2,m)} = K_{pc}C_{g(2,m)}.$$

The Mucus/Tissue Compartment

The transport through the N nodes of each of the M sections of the tissue compartment was assumed to occur through molecular diffusion. The basic equation for this is

$$dC/dt = D\partial^2C/\partial L^2,$$

where D is the molecular diffusivity (m^2/sec) of the diffusing species and L is the parameter length (m). This equation was solved numerically for each M tissue section by using a simple explicit finite difference scheme given by Crank (1975, p. 142). Discrete tissue concentrations were calculated for each of the $M \times N$ nodes and were stored in the matrix $C_{(N,2,M)}$. Index 2 refers to the concentrations of two adjacent time steps necessary to store when using the chosen numerical method.

The concentration in the M boundary elements at the air interface after the lapse of one time step is given by

$$C_{(0,2,m)} = C_{(0,1,m)} + 2R(C_{(1,1,m)} - C_{(0,1,m)}).$$

where $R = Ddt/dL^2$. Similarly, for the second through $(N-1)$th nodes through the tissue is obtained by

$$C_{(n,2,m)} = C_{(n,1,m)} + 2R(C_{(n-1,1,m)} - 2C_{(n,1,m)} + C_{(n+1,1,m)}),$$

and finally, for the Nth node at the blood boundary, the new concentration is given by

$$C_{(N,2,m)} = C_{(N,1,m)} + 2R(C_{(N-1,1,m)} - C_{(N,1,m)}).$$

The Blood Compartment

The vapor concentration in the exiting blood was assumed to be in equilibrium with

the local neighboring tissue element in the nasal mucosa, and the tissue/blood partition coefficient is assumed to be 1. After the lapse of one time step, the blood flow causes a change in the concentration of the neighboring tissue elements according to

$$C_{(N,2,m)} = C_{(N,1,m)} \Big/ \left(1 + \frac{2Q_b dt}{dL}\right).$$

The Coupling Equations and Uptake Calculations

The equations of the three different compartments were coupled by use of time splitting or the method of fractional steps (Press *et al.*, 1986). For each time step, the concentrations of the M sections of the airspace compartment and the M concentrations of the exiting blood were solved. This simultaneously gave the new concentrations of the two times M boundary nodes of the mucus/tissue compartment. The concentrations of the mucus/tissue nodes then were solved for the same time step. After replacing all old concentrations with the new ones, the procedure was repeated.

The simulations were run for eight full-breathing cycles, and sampling for calculating absorption, desorption, and uptake was made during the last cycle. Concentrations at corresponding locations and phase angles were compared during the last two cycles, and a mass balance was calculated for the last cycle.

The number of sections and nodes of the model were increased until no further improvement of the mass balance was obtained, and no significant differences in concentrations at corresponding positions were observed. This required 20 sections with 21 nodes each in the mucus/tissue compartment. To give a stable solution and an accurate mass balance, 48,000 time steps were required.

ACKNOWLEDGMENT

We thank Drs. B. R. Scott and R. F. Henderson for their critical review of this paper. This research was supported by the National Institute of Environmental Health Sciences Grant ES04422 and by the Office of Health and Environmental Research of the U.S. Department of Energy in facilities provided by the Office of Health and Environment Research of the U.S. Department of Energy under Contract DE-AC04-76EV01013. One of the authors, Per Gerde, was a postdoctoral participant during the conduct of this research and was sponsored by the Swedish Work Environment Fund through Grant 88-1255.

REFERENCES

ADAMS, D. R., AND HOTCHKISS, D. K. (1983). The canine nasal mucosa. *Zbl. Vet. Med. C. Anat. Histol. Embryol.* **12,** 109–125.

AHARONSON, E. F., MENKES, H., GURTNER, G., SWIFT, D. L., AND PROCTOR, D. F. (1974). Effect of respiratory airflow rate on removal of soluble vapors by the nose. *J. Appl. Physiol.* **37,** 654–657.

BAILEY, M. R. (1984). Assessment of the dose to the nasopharyngeal region from inhaled radionuclides. In *Lung Modelling for Inhalation of Radioactive Materials* (H. Smith and G. Gerber, Eds.), pp. 273–278. National Radiation Protection Board, Oxford, UK.

BIRD, R. B., STEWART, W. E., AND LIGHTFOOT, E. N. (1960). *Transport Phenomena.* Wiley, New York.

BRAIN, J. D. (1970). The uptake of inhaled gases by the nose. *Ann. Otol. Rhinol. Laryngol.* **79,** 529–539.

CORN, M., KOTSKO, N., AND STANTON, D. (1976). Mass-transfer coefficient for sulphur dioxide and nitrogen dioxide removal in cat upper respiratory tract. *Ann. Occup. Hyg.* **19,** 1–12.

CRANK, J. (1975). *The Mathematics of Diffusion,* pp. 44–68. Oxford Univ. Press (Clarendon), London/New York.

DAHL, A. R. (1990). Dose concepts for inhaled vapors and gases. *Toxicol. Appl. Pharmacol.* **103,** 185–197.

DAHL, A. R., SNIPES, M. B., AND GERDE, P. (1991). Sites for uptake of inhaled vapors in Beagle dogs. *Toxicol. Appl. Pharmacol.* **109,** 263–275.

DAVIDSON, M. R., AND SCHROTER, R. C. (1983). A theoretical model of adsorption of gases by the bronchial wall. *J. Fluid Mech.* **129,** 313–335.

DUBOIS, A. B., AND ROGERS, R. M. (1968). Respiratory factors determining the tissue concentrations of inhaled toxic substances. *Respir. Physiol.* **5,** 34–52.

GUILMETTE, R. A., WICKS, J. D., AND WOLFF, R. K. (1989). Morphometry of human nasal airways *in vivo* using magnetic resonance imaging. *J. Aerosol Med.* **2,** 365–377.

HANNA, L. M., FRANK, R., AND SCHERER, P. W. (1985). Absorption of soluble gases and vapors in the respiratory system. In *Gas Mixing and Distribution in the Lung* (Pavia and Engel, Eds.), pp. 277–316. Dekker, New York.

HANNA, L. M., AND SCHERER, P. W. (1986). Measurement of local mass transfer coefficients in a cast model of the

human upper respiratory tract. *J. Biomech. Eng.* **108,** 12–18.

HENDERSON, Y., AND HAGGARD, H. W. (1943). *Noxious Gases and The Principles of Respiration Influencing Their Action,* pp. 110–123. Reinhold, New York.

LABELLE, C. W., LONG, J. E., AND CHRISTOFANO, E. E. (1955). Synergistic effects of aerosols. *Arch. Ind. Health* **11,** 297–304.

LIGHTFOOT, E. N. (1974). *Transport Phenomena and Living Systems.* Wiley, New York.

MILLER, F. J., OVERTON, J. H., JASKOT, R. H., AND MENZEL, D. B. (1985). A model of the regional uptake of gaseous pollutants in the lung. I. *Toxicol. Appl. Pharmacol.* **79,** 11–27.

MORGAN, M. S., AND FRANK, R. (1977). Uptake of pollutant gases by the respiratory epithelium. In *Respiratory Defense Mechanisms* (J. D. Brain, D. F. Proctor, and L. M. Reid, Eds.), pp. 157–189. Dekker, New York.

MORGAN, K. T., AND MONTICELLO, T. M. (1990). Airflow, gas deposition, and lesion distribution in the nasal passages. *Environ. Health Perspect.* **88,** 209–218.

MORRIS, J. B., AND CAVANAGH, D. G. (1986). Deposition of ethanol and acetone vapors in the upper respiratory tract of the rat. *Fundam. Appl. Toxicol.* **6,** 78–88.

MUGGENBURG, B. A., AND MAUDERLY, J. L. (1974). Cardiopulmonary function of awake, sedated, and anesthetized dogs. *J. Appl. Physiol.* **37,** 152–157.

OVERTON, J. H. (1984). Physicochemical processes and the formulation of dosimetry models. *J. Toxicol. Environ. Health* **13,** 273–294.

PERRY, R. H., CHILTON, C. H., AND KIRKPATRICK, S. D. (1963). *Chemical Engineers' Handbook.* McGraw-Hill, New York.

PEFFER, M. A., AND FROHLICH, E. D. (1972). Electromagnetic flowmetry in anesthetized rats. *J. Appl. Physiol.* **33,** 137–140.

PRESS, W. H., FLANNERY, B. P., TEULKOLSKY, S. A., AND VETTERLING, W. T. (1986). *Numerical Recipes,* pp. 615–672. Cambridge Univ. Press, Cambridge.

PROCTOR, D. F., AND SWIFT, D. L. (1977). Temperature and water vapor adjustment. In *Respiratory Defense Mechanisms* (J. D. Brain, D. F. Proctor, and L. M. Reid, Eds.), pp. 95–124. Dekker, New York.

SATO, A., AND NAKAJIMA, T. (1979). Partition coefficients of some aromatic hydrocarbons and ketones in water, blood and oil. *Br. J. Ind. Med.* **36,** 231–234.

SCHREIDER, J. P., AND RAABE, O. G. (1981). Anatomy of the nasal–pharyngeal airway of experimental animals. *Anat. Rec.* **200,** 195–205.

SCOTT, W. R., TAULBEE, D. B., AND YU, C. P. (1978). Theoretical study on nasal deposition. *Bull. Math. Biol.* **40,** 581–603.

SNIPES, M. B., SPOO, J. W., BROOKINS, L. K., JONES, S. E., MAUDERLY, J. L., ORWAT, T. B., STIVER, J. H., AND DAHL, A. R. (1990). A method for measuring nasal and lung uptake of inhaled vapor. *Fundam. Appl. Toxicol.* **16,** 81–91.

STOTT, W. T., RAMSEY, J. C., AND MCKENNA, M. J. (1986). Absorption of chemical vapors by the upper respiratory tract of rats. In *Toxicology of the Nasal Passages* (C. S. Barrow, Ed.), pp. 191–210. Hemisphere, New York.

ULTMAN, J. S. (1986). Transport and uptake of inhaled gases. In *Air Pollution, The Automobile, and Public Health* (A. Y. Watson, R. R. Bates, and D. Kennedy, Eds.), pp. 323–366. National Academy Press, Washington.

YEH, H. C. (1974). Use of a heat transfer analogy for a mathematical model of respiratory tract deposition. *Bull. Math. Biol.* **36,** 105–116.